Journal of Fluorescence, Vol. 8, No. 4, 1998

Fluorescence Investigations of "Smart" Microgel Systems

N. J. Flint,[1] S. Gardebrecht,[1] and L. Swanson[1,2]

Received January 25, 1998; Accepted July 17, 1998

Fluorescence techniques, including lifetime, quenching, and time-resolved anisotropy measurements (TRAMS), were used to study microgel systems based upon *N*-isopropylacrylamide (NIPAM) using pyrene as a fluorescent probe. These experiments have revealed that poly(*N*-isopropylacrylamide) (PNIPAM) nanoparticles undergo a phase transition at a lower critical solution temperature (LCST), of ca. 34°C, which involves collapse of the particles into compacted, hydrophobic spheres. A degree of control over the LCST has been achieved by copolymerization of NIPAM with varying amounts of dimethylacrylamide (DMAC). Incorporation of DMAC into the gel has the effect of changing the hydrophobic to hydrophilic balance and shifts the LCST to a higher temperature. Fluorescence methods indicate that the NIPAM/DMAC gels are of a more open, water-swollen nature above the LCST than that of their PNIPAM counterparts.

KEY WORDS: Microgels; *N*-isopropylacrylamide; time-resolved anisotropy.

INTRODUCTION

The last decade has witnessed an enormous expansion in the literature regarding the use of luminescence spectroscopy to probe the conformational behavior of water-soluble polymers. (See, for example, Refs. 1–9 and references therein.) Several research groups have championed its value as a tool which not only allows investigation of a diversity of systems but also bridges a vast concentration range, from the ultradilute regime through to highly concentrated samples. As researchers endeavor to solve the problems of ever more complex macromolecular assemblies, so luminescence techniques enjoy increasing exposure to yet more diverse systems. In a continuation of this theme, we report, in this paper, on the use of fluorescence methods to characterize microgels (aqueous dispersions of cross-linked polymer particles) based on poly(*N*-isopropylacrylamide) (PNIPAM).

PNIPAM is known as a "smart" polymer. It exhibits thermoreversible phase-separation behavior in aqueous solution [10] and is characterized by a lower critical solution temperature (LCST) of 31–32°C [10,11]. The implication of this property is that above the LCST (under semidilute conditions), it forms a turbid solution which *rapidly* turns clear again upon cooling. The LCST phenomenon requires the existence of specific interactions between the polymer and the solvent which result in *both* a negative enthalpy change, ΔH_m, upon mixing and a negative entropy change, ΔS_m. Furthermore, the relative magnitudes of ΔH_m and ΔS_m must be such as to effect reversal of the sign of the free energy change, ΔG_m, for the mixing process, within the range of temperatures over which the solvent remains a liquid

The LCST behavior of PNIPAM has prompted interest from several photophysics groups who have utilized energy transfer experiments [12] and time-resolved anisotropy measurements (TRAMS) [13,14] to monitor phase separation in the polymeric dispersions. As a result of these investigations, a mechanism has been proposed in an attempt to describe the thermoreversible behavior of PNIPAM: initially, the polymer undergoes a conformational transition from a flexible coil to a glob-

[1] School of Physics and Chemistry, Lancaster University, Lancaster LA1 4YA, UK.
[2] To whom correspondence should be addressed.

1053-0509/98/1200-0343$15.00/0

ular structure. This is followed, subsequently, by *inter*-molecular aggregation between collapsed coils. It is the latter feature of the process which confers rapid reversibility upon the phase separation behavior. The thermoresponsivity of PNIPAM has aroused much interest in researchers hoping to generate "smart" materials with temperature-sensitive permeability characteristics. Examples of such intelligent systems include membranes, capsules, and microgels [11,15–17]. Microgels are materials which, in particular, have received increasing attention in this respect.

Microgels consist of cross-linked polymer colloids of micrometer dimensions which are very important in technologies relying on solubilization and lubrication phenomena [16,18]: they are used, for example, in paints (as rheology modifiers), oil products, drug release systems, and foods. The microgels which have been synthesized to date are based largely on PNIPAM: particles consisting of cross-linked PNIPAM are consequently thermoresponsive when dispersed in water, shrinking and swelling reversibly with changing temperature [16–18]. Techniques which have proved useful in monitoring such behavior include DSC [19], NMR [20], and light scattering [18].

The conformational collapse which occurs in the PNIPAM microgels upon increasing the temperature beyond 32°C allows the particles to absorb materials with differing efficiencies above and below the LCST. (Solutes can be released again by lowering the temperature below the LCST.) It is this (reversible) feature which has aroused interest in nanoparticles for use as drug uptake and release systems [18]. In light of this, researchers have attempted to modify microgels in order to change their affinity for certain solutes. For example, previous research has indicated [16,21] that heavy-atom nitrates are sequestered into the particles in the expanded form and released to the aqueous phase on contraction of the colloids at higher temperature. Variation of the initiator used in the polymerization allows preparation of materials with sulfonate, carboxylate or cationic surface groups [21]. This in turn, can significantly change the degree of uptake of ions from solution [16,21], which may be of importance in the treatment and purification of water, for example.

Shibayama *et al.* [17] have shown, using DSC, that a degree of control over the LCST can be achieved by modification of the PNIPAM-based microgels with monomers such as acrylic acid (AA) and dimethylacrylamide (DMAC). However, it was found that copolymerization can cause a significant reduction in the magnitude of the enthalpy change which characterizes the transition from compact to open structure and, in the case of AA-modified microspheres, induces a pH and salinity dependence, in addition to that upon temperature [17]. In the light of these observations, it is appropriate to assess the effects of alteration of the hydrophobic/hydrophilic balance of these systems upon the nature of the microgels and their solubilization capacities, below and above their LCSTs. We have used photophysical probing to study these effects.

To date, luminescence spectroscopy has not featured prominently in determining the physical characteristics of microspheres [22]. In this paper, we present examples of the types of fluorescence experiment which can provide information regarding the thermoreversible behavior and morphology of PNIPAM-based microgels. We also report upon nanoparticles containing NIPAM which have been modified with varying amounts of DMAC in order to induce a degree of control over the LCST.

EXPERIMENTAL

Materials

N-Isopropylacrylamide (NIPAM; Aldrich; 97%) was purified by multiple recrystallization from a mixture (60/40%) of toluene and hexane (both spectroscopic grade; Aldrich).

Ammonium persulfate (APS; Aldrich; 99%), sodium lauryl sulfate (SDS; Aldrich; 99%), *N,N'*-methylenebisacrylamide (MBA; BDH; electrophoresis grade), and *N,N,N'N'*-tetramethylethylenediamine (TMED; Lancaster Synthesis; 99%) were used as received.

Dimethylacrylamide (DMAC; Aldrich; 99%) was vacuum distilled prior to use. Pyrene (Aldrich; 99%) was recrystallized five times from spectroscopic-grade toluene.

Microgel samples containing varying amounts of NIPAM and DMAC were prepared in a single-step emulsion polymerisation process in double-distilled, degassed water at 25°C, in the presence of *N,N'*-methylenebisacrylamide as cross-linker: the total aqueous charge of the system was 600 cm^3 and contained 8.25 g of monomer (including MBA) in total. The APS (0.6 g)/TMED (0.3 g) initiator system was used to initiate the polymerization. HCl (0.5 *M*, 20 ml) was added to terminate the reaction after 55 min. All microgel samples were purified by dialysis. Details of the various feed compositions and solids contents are given in Table I.

The LCST behavior of the various microgels was determined by cloud point measurements (through visual

Table I. Details of Microgel Compositions and LCSTs

System	NIPAM (wt %)[a]	DMAC[a]	wt % solids[b]	LCST (°C)[c]
PNIPAMμgel	90.9	—	1.32	34
NIPAM–DMAC(4)μgel	87.3	3.6	1.35	40
NIPAM–DMAC(16)μgel	74.5	16.4	1.33	45
NIPAM–DMAC(31)μgel	59.9	31.0	1.34	51

[a] Feed content with respect to the total monomer.
[b] Solids content following dialysis.
[c] Determined by cloud-point measurements.

observation of the onset of turbidity). The resulting onset temperatures are listed in Table I for each sample.

Solutions for spectroscopic analysis contained ca.0.13 wt% microgel and 10^{-6} *M* pyrene.

Instrumentation

Steady state-fluorescence spectra (uncorrected for wavelength dependence of excitation source intensity and instrument response) were measured on a Perkin–Elmer LS50 spectrometer.

Fluorescence lifetime data were acquired on an IBH System 5000 time-correlated single-photon counter, employing D_2 as a discharge medium in the nanosecond flashlamp used as the pulsed excitation source.

Time-resolved anisotropy measurements (TRAMS) were carried out on a specially modified Edinburgh Instruments 199 time-correlated single-photon counter, vertically polarized light was used to excite the sample and fluorescence intensities transmitted by a polarizer were analyzed in planes parallel, $I_{\|}(t)$, and perpendicular, $I_{\perp}(t)$, to that of the polarized excitation. An automated "toggling procedure" was employed in the collection of $I_{\|}(t)$ and $I_{\perp}(t)$ wherein the analyzer was sequentially altered while memory quarters in the multichannel analyzer were switched simultaneously.

RESULTS AND DISCUSSION

Steady-State Fluorescence Spectra

It is well known that the fluorescence spectrum of pyrene is sensitive to the polarity of its environment [23,24]: the ratio of the intensity of the third vibronic band (I_3) to the first (I_1) changes in solvents of differing polarity. As a consequence, there are many examples cited in the literature of the use of pyrene as a probe of hydrophobicity in a variety of aqueous borne polymer systems and in other organized media. Indeed, such applications are discussed in detail in a recent excellent review [25].

Figure 1 shows the excitation and emission spectra of 10^{-6} *M* pyrene dispersed within PNIAPMμgel (0.13 wt%) at 20 and 48°C, respectively. The fluorescence spectrum both above (48°C) and below (20°C) the LCST is characteristic of that of monomeric, unassociated pyrene: there is no spectroscopic evidence for excimer formation under the conditions of concentration and temperature employed. The I_3/I_1 ratio at 20°C (ca. 0.55) is similar to that in water [22,26,27], which indicates that the probe is in an isolated aqueous-rich phase. Such behavior would be expected below the LCST since the microgel is in its expanded form in which its interstitial pockets are filled with water. Further reference to Fig. 1 reveals that at 48°C there is a marked change in the spectrum compared to that at 20°C: the I_3/I_1 ratio increases to ca. 0.7. (In this respect, the current pyrene spectroscopic data follow similar trends to those observed in a previous study upon PNIPAM microgels [22]).

A slight red shift is evident in *both* the excitation and the emission spectra above the LCST when compared to that at 20°C. Similar behavior has been reported [25] in systems in which excimer formation involving "preassociated" pyrenes occurs and also when probes are solubilized within the hydrophobic cavities of certain water-soluble polymers [27]. In the latter instance, spectral shifts were considered indicative of pyrene molecules residing in a solvating hydrophobic-rich medium. Since there is no evidence of excimer formation in the current work, it seems likely that the spectral shifts reflect the fact that above the LCST, the particles collapse, solubilizing the probes into hydrophobic domains in the process.

The I_3/I_1 ratio is plotted in Fig. 2 as a function of temperature for pyrene dispersed within the PNIPAMμgel sample and the various DMAC-modified microgels. With reference to Fig. 2, it is apparent that the following apply for the PNIPAMμgel:

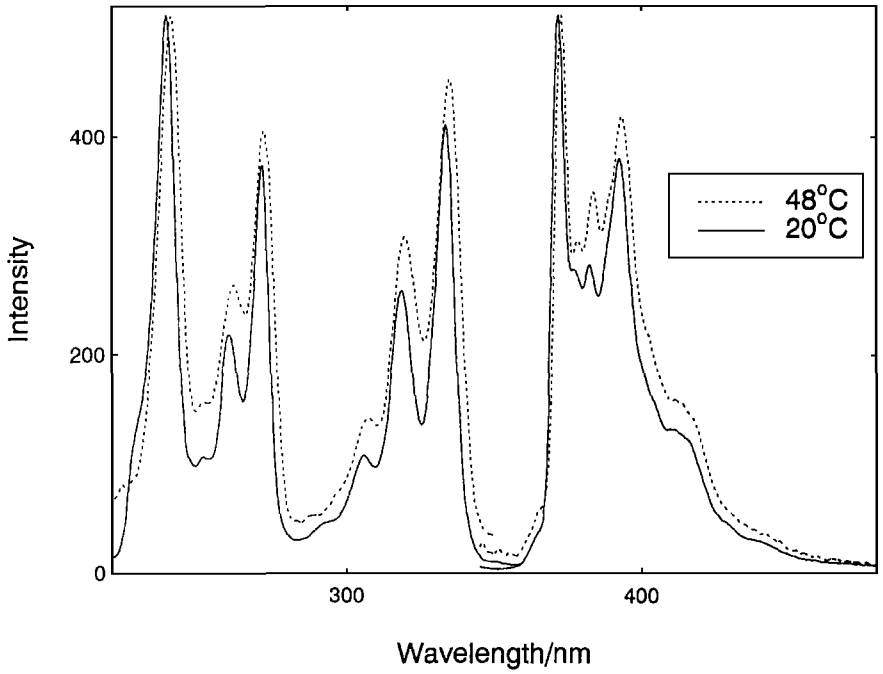

Fig. 1. Fluorescence excitation and emission spectra for pyrene (10^{-6} *M*) dispersed in PNIAPMμgel (0.13 wt%) at 20°C (–) and 48°C (–), respectively. λ_{ex} = 335 nm; λ_{em} = 370 nm.

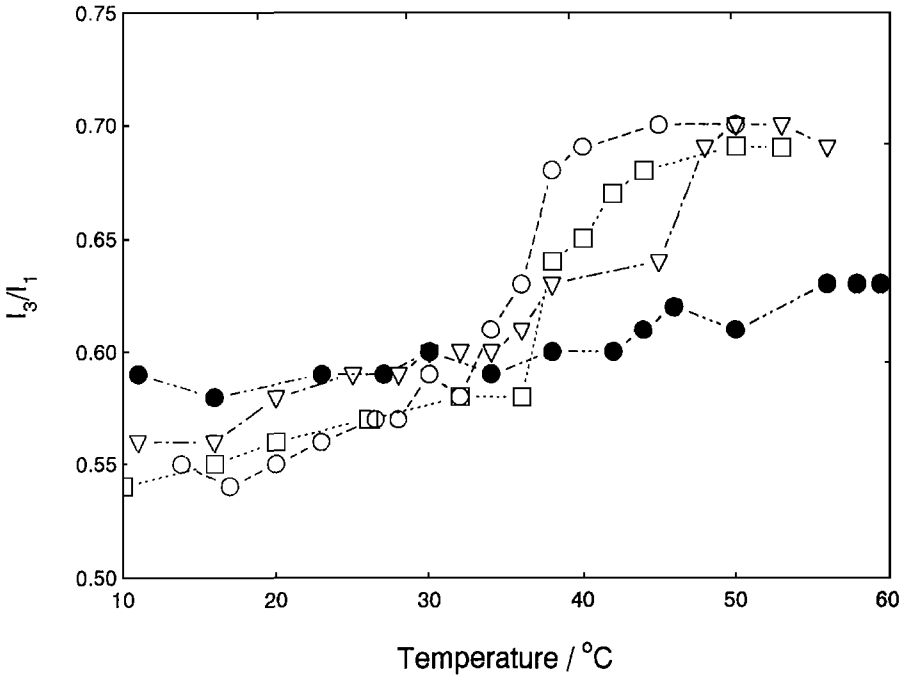

Fig. 2. I_3/I_1 ratios from the fluorescence spectra of pyrene (10^{-6} *M*) dispersed in various microgels (0.13 wt%) as a function of temperature. (○) PNIPAMμgel; (□) NIPAM-DMAC(4)μgel; (▽) NIPAM-DMAC(16)μgel; (●)NIPAM-DMAC(31)μgel.

(i) The polarity of the microenvironment sensed by the dispersed probe depends upon the temperature of the system. The dependence of I_3/I_1 upon temperature acts as a clear monitor of the collapse of the microgel: from low temperatures where the probe resides in the water-swollen, expanded phase to the hydrophobic confines of the collapsed gel above the LCST.

(ii) A clear discontinuity in the I_3/I_1 vs temperature profile is apparent at ca. 36°C. This is close to that at which phase separation occurs as determined by cloud point measurements (cf. Table I) and presumably marks the onset of the LCST.

Modification of the microgels using DMAC leads to the generation, at higher temperatures, of particles capable of solubilizing pyrene [i.e., the I_3/I_1 ratios for NIPAM–DMAC(16)μgel and NIPAM-DMAC(4)μgel are ca. 0.7 at temperatures in excess of 50°C). However, a shift in the onset temperature of the discontinuity in I_3/I_1 is apparent: the greater the DMAC content, the higher the temperature at which the particles collapse.

Furthermore, the following is evident.

(a) When the DMAC content is high (e.g., 31 wt%, with respect to the total monomer), the polarity of the gel in the collapsed form is greater than that of the PNIPAMμgel. This provides an early indication that NIPAM–DMAC(31)μgel at 50°C affords pyrene with a more aqueous-rich environment than that of PNIPAMμgel at the same temperature.

(b) Below the LCST for each of the gels in the current study, there is evidence that the probe senses a slightly different polarity in the expanded forms on increasing the DMAC content: the I_3/I_1 ratio at 20°C increases from ca. 0.55 for the PINPAMμgel to ca. 0.59 for the NIPAM–DMAC(16)μgel sample.

Although the spectroscopic data serve as a crude indicator of the hydrophobicity of the various microgels, fluorescence lifetime measurements (as discussed below), coupled with quenching experiments (see later), prove to be more informative as regards particle morphology.

Fluorescence Lifetime Measurements

The singlet excited-state lifetime of pyrene is sensitive to the polarity of the medium in which it is dispersed [28]. This property has been widely used by many researchers interested in studying the conformational behavior of water-soluble polymers [2,27,29,30]. In a similar manner, the fluorescence lifetime of pyrene can be used to monitor the collapse and expansion of the various microgel samples and, thus, to determine the LCST.

Fluorescence lifetime measurements were made on pyrene dispersed within the various microgels as a function of temperature. Below the LCST, the emission from each sample could be adequately described, on statistical grounds, through use of a single-exponential function of the form

$$I(t) = I_o \exp(-t/\tau) \quad (1)$$

A common "lifetime" of ca. 130 ns for each of the nanoparticle/pyrene dispersions, at 25°C, was consistently recovered by this form of analysis. This value is very similar to that of pyrene in water (130 ± 5 ns) [27] and infers that, below the LCST, each gel presents the probe with a solvent environment similar to that of the bulk aqueous phase. (Such would be expected of the expanded, water-swollen morphologies that are believed to characterize PNIPAM microgels below the LCST.)

At temperatures above that of the LCST, for each particular microgel, the decays of fluorescence from the pyrene probe become too complex for adequate description in terms of a single-exponential function. Dual-exponential analyses of the form of equation (2), on the other hand,

$$I(t) = I_1 \exp(-t/\tau_1) + I_2 \exp(-t/\tau_2) \quad (2)$$

do result in fits to the observed emissions that are justified on statistical grounds. While this could be taken as indictative of the fact that the pyrene guest can be located in either of two environments (an aqueous-rich phase and a polymer-rich hydrophobic domain), it is more likely that the dual-exponential modeling function merely serves to parameterize, in a statistically adequate fashion, fluorescence originating from a broad heterogeneous range of environments. Indeed, it has been argued [8,27] previously that ascribing [2,29,30] such components to pyrene chromophores solubilized in polar environments and occluded within more hydrophobic phases of water-soluble polymers, respectively, is probably an oversimplification: it was considered unlikely [8,27] that these two populations are sufficiently distinct, within the overall distribution of dispersed probes, to be resolved by such analysis. It is conceivable that the pyrene data for each of the samples above the LCST in the current microgel systems may also suffer from mere parameterization when more complex fitting functions are adopted and, as such, may not provide any further information regarding particulate morphology.

Alternatively, in a bid to accommodate such problems, the "lifetime" resultant from single-exponential analyses can be used as a simple monitor of the ther-

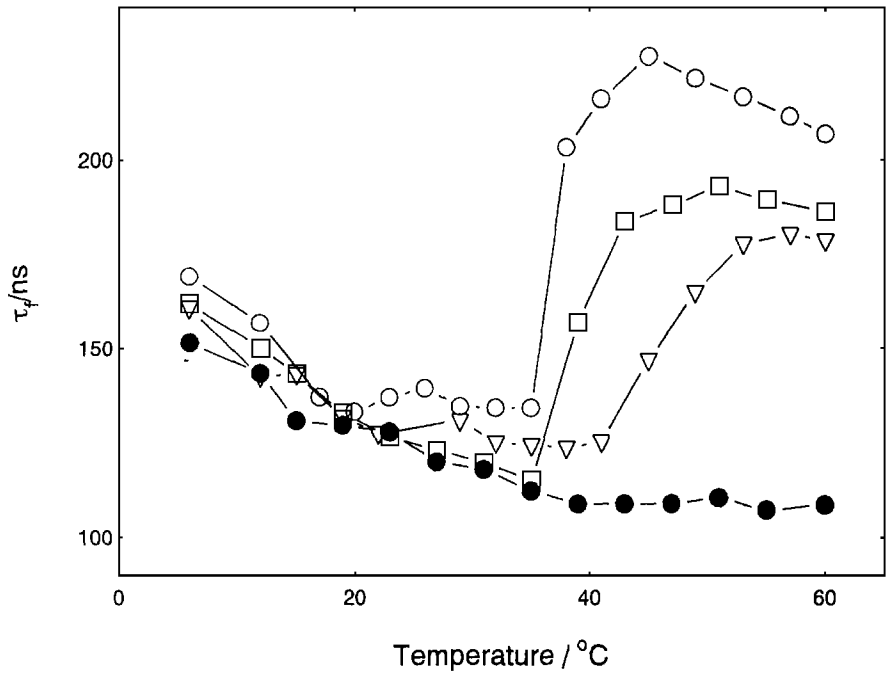

Fig. 3. Fluorescence lifetime of pyrene (10^{-6} *M*) dispersed in various microgels (0.13 wt%) as a function of temperature. (○) PNIPAMμgel; (□) NIPAM-DMAC(4)μgel; (▽) NIPAM-DMAC(16)μgel; (●)NIPAM-DMAC(31)μgel.

moresponsive behavior of each of the microgel samples as shown in Fig. 3.

With reference to Fig. 3 it is apparent that the excited-state lifetime of pyrene, when dispersed in PNIPAMμgel, undergoes a marked increase at ca. 38°C: from ca. 130 ns at 25°C to in excess of 200 ns beyond the LCST. Presumably this reflects encapsulation of the probe into the hydrophobic confines of the domains formed upon collapse of the particles. (These observations are consistent with the findings based upon the I_3/I_1 data discussed in the previous section.) Both above and below the respective LCSTs for each of the samples in the current study, the lifetime data show a more conventional trend: the higher the temperature, the shorter the lifetime.

Further reference to Fig. 3 reveals the following.

(i) Increasing the DMAC content within the microgel shifts the onset of the conformational collapse (and hence the LCST) to higher temperature. (These observations are also in agreement with the spectroscopic data discussed earlier.)

(ii) The magnitude of the conformational transition (as reflected by the change in fluorescence lifetime) decreases as the DMAC content increases.

(iii) The lifetime of pyrene dispersed within the highest DMAC content sample [NIPAM–DMAC(31)μgel] at any temperature between 5 and 60°C is similar to that in water: this infers that *if* this microgel has any solubilization capacity at all for pyrene, it presents the probe with a solvent environment similar to that of the bulk aqueous phase.

Clearly, DMAC-modification of the PNIPAM particles results in a change in the hydrophobic to hydrophilic balance within the microgel which serves to shift the LCST to higher temperature. (The principles involved in achieving and controlling LCST behavior in water-soluble polymers are well established. The interested reader is directed to reference 15 for a comprehensive review of the subject.) Similar findings regarding the effects of incorporation of DMAC into the microgels upon both the LCST and the "intensity" of the transition were reported [17] in an earlier study. The current spectroscopic probe data demonstrate that the calorimetric observations, of a reduction in the endotherm associated with the collapse of the microgel, as the DMAC content of the system is increased, reflects a concomitant change in the nature of the colloidal particle above its LCST. Fluorescence quenching experiments, described below, support this inference.

Fluorescence Quenching Measurements

Fluorescence quenching experiments can, in principle, provide information regarding the degree of access afforded to a label or probe by a small molecule quencher. This, in turn, reflects the "openness" or "compactness" of a polymer coil, for example. There are many cases cited in the literature of the use of quenching measurements to investigate the conformational behaviour of water-soluble polymers [2–4,8]. Recent reports have also featured the technique as a means of probing the morphologies of more complex systems such as water-dispersible [31–33] and swellable colloids [22]. In order to investigate further the LCST behavior of our various microgel samples, quenching experiments were carried out using nitromethane as a water-soluble, uncharged quencher.

For a purely dynamic quenching mechanism, the Stern–Volmer equation relates the intensity of fluorescence, I^0 (or the lifetime, τ^0) in the absence of quencher, to that [$I(\tau)$] in the presence of some concentration of quencher [Q] as follows,

$$I^o/I = \tau^o/\tau = 1 + k_q \tau^o [Q] \quad (3)$$

where k_q is the bimolecular quenching constant. In our experience, the use of nitromethane as a quencher is generally attended by the influence of static components to the quenching mechanism. (See, for example, Refs. 8 and 33.) This invalidates the use of steady-state fluorescence intensity data in the estimation of k_q. Consequently, we have used fluorescence lifetime data, which reflect purely dynamic quenching, in our estimates of k_q.

Fluorescence decay data from pyrene dispersed within each of the microgel systems were acquired at various concentrations of nitromethane at 298 and 330 K, respectively. For all Stern–Volmer experiments the transient behavior of the probe was modeled in terms of a single-exponential function of the form of Eq. (1). Typical data are presented in Fig. 4. The resultant k_q values are listed in Table II.

Reference to Table II reveals that for the PNIPAM microgel below its LCST (298 K), the efficiency of quenching is very high: a bimolecular quenching constant of ca. $8 \times 10^9\ M^{-1}\ s^{-1}$ results. This value is close to that expected for a diffusion controlled process in aqueous media and implies that the probe is

(i) in a very fluid environment and

(ii) within a very exposed or accessible phase.

These observations are consistent with those based upon the unquenched lifetime data (discussed earlier) since they infer that, below the LCST, the pyrene is located either in the aqueous phase or within the expanded, water-swollen microgel. Above the LCST (at 330 K) the degree of quenching is markedly reduced: a k_q value of ca. $1.0 \times 10^8\ M^{-1}\ s^{-1}$ results. Clearly, the quencher experiences greater difficulty in accessing the probe dispersed within the collapsed form of the microgel.

The quenching data obtained for PNIPAMμgel, in the current study, follow trends similar to those obtained in an earlier report [22]. However, in the earlier study [22], the lifetime data above the LCST were modeled by a double-exponential function of the form of Eq. (2). It was assumed [22] that two distinct populations of pyrene exist within the microgel: it was proposed [22] that one distribution is associated with probes located within the aqueous phase, while the second is considered to reflect fluors occluded within the hydrophobic confines of the collapsed nanoparticle. Consequently, it was argued [22] that two quenching constants would best describe the data above the LCST: the first would reflect the inaccessibility of the core of the collapsed gel, while the second would be consistent with quenching in the more exposed, aqueous phase.

There are problems associated with such an approach. First, there is the assumption that the two fluorescence lifetime parameters recovered in adoption of a dual exponential model function in analysis of the decays of fluorescence from the pyrene probe truly represent pyrenes located in the microgel and bulk aqueous phases, respectively. As we discussed above, it is possible that such dual-exponential fitting may serve merely to parameterize, in a statistically adequate fashion, fluorescence emanating from a distribution of environments in which the pyrene is dispersed between the polymer-rich and the aqueous-rich phases which exist above the LCST. However, there is also a second assumption involved: it must be assumed that the quencher is equipartitioned between the "two" phases [since the quenching of a given chromophore component will be governed by the (unknown) "local" concentration of quencher, rather than its overall concentration in the system].

In view of these potential problems, and bearing in mind that we seek only to establish the creation (or otherwise) of markedly different microphases above and below the LCST of each of the microgels under investigation, we have analyzed our decay data in terms of a single exponential model of the form of Eq. (1).

Table II also lists k_q values for each of the various DMAC-modified microgels below (298 K) and above (330 K) their respective LCSTs. Clearly, by reference to Table II, it can be concluded that the degree of quenching in each of the gel systems is the same (within experimental error) as that of diffusion control within an

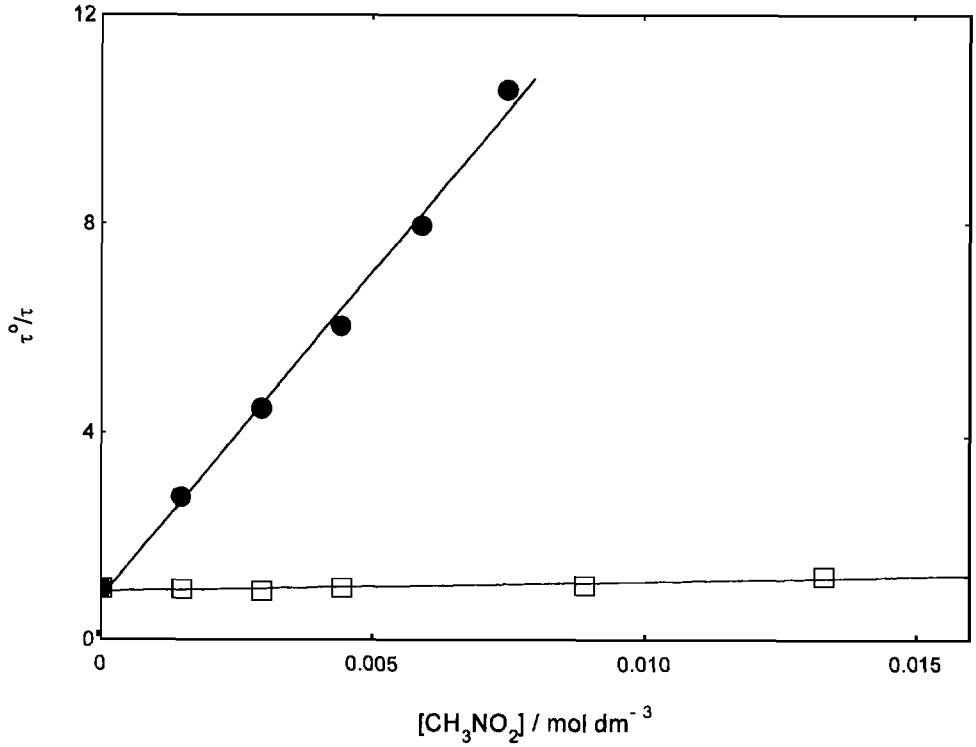

Fig. 4. Stern–Volmer plots for nitromethane-induced quenching of the excited state lifetime of pyrene dispersed in PNIPAM microgel (0.13 wt%) at 298K (●) and 330K (□).

Table II. Bimolecular Quenching Constants Obtained for the Various Microgels

	$k_q \times 10^9$ (M^{-1} s^{-1})	
Sample	298 K	330 K
PNIPAMμgel	8.8	0.1
NIPAM–DMAC(4)μgel	6.3	0.2
NIPAM–DMAC(16)μgel	7.2	1.1
NIPAM–DMAC(31)μgel	6.7	4.4

aqueous medium (ca. 10^{10} M^{-1} s^{-1}) at 298 K. However, consideration of the data above the LCST (cf. Table II) reveals that the quenching efficiencies vary from one system to another: clearly, increasing the DMAC content within the nanoparticle increases the degree of access by the CH_3NO_2 to the probe and, in turn, the degree of quenching. For example, the sample containing the highest DMAC content, NIPAM–DMAC(31)μgel, has the largest bimolecular rate constant (ca. 4×10^9 $M^{-1}s^{-1}$) at 330 K. This implies that the pyrene is

(i) located within an exposed/accessible phase and
(ii) dispersed within a fluid medium.

These data support the lifetime and spectroscopic evidence (i.e., I_3/I_1 ratios) discussed earlier in that increasing the DMAC content results in a more open, water-swollen microgel structure above the LCST. These results also support the findings of a previous report [17] which used DSC and light-scattering measurements to investigate the effect of DMAC modification of PNIPAM-based microgels.

Time-Resolved Anisotropy Measurements

The observed anisotropy, $r(t)$, can be constructed from its fluorescence components via the relationship

$$r(t) = \frac{I_{\parallel}(t) - I_{\perp}(t)}{I_{\parallel}(t) + 2I_{\perp}(t)} \quad (4)$$

where $I_{\parallel}(t)$ and $I_{\perp}(t)$ are the time-dependent intensities of emission detected in planes parallel and perpendicular, respectively, to that of vertically polarized excitation.

If the decay of anisotropy is due to a simple, single relaxation process, then $r(t)$ can be described by Eq. (5):

$$r(t) = r_0 \exp(-t/\tau_c) \quad (5)$$

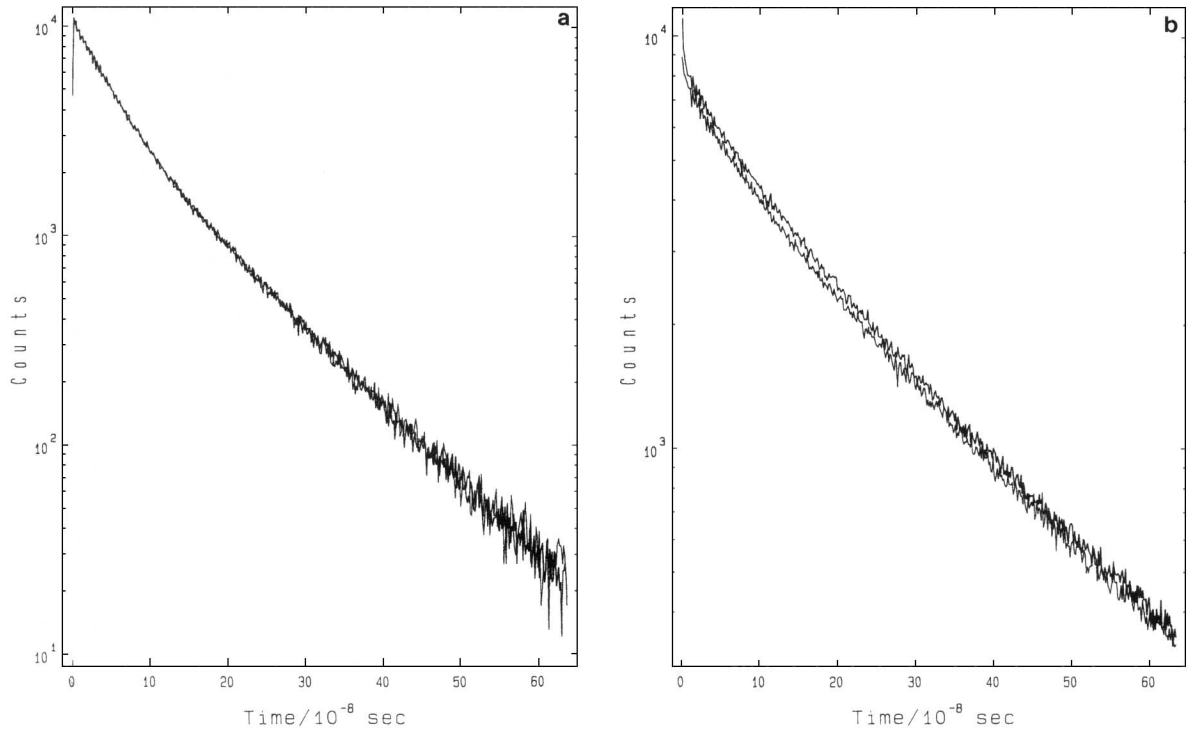

Fig. 5. $I_{\parallel}(t)$ (upper curve) and $I_{\perp}(t)$ decay curves (λ_a = 370 nm), following vertically polarized excitation (λ_{ex} = 335 nm) of pyrene dispersed in PNIPAMμgel (0.13 wt%) at (a) 25°C and (b) 51°C.

where r_o is the intrinsic anisotropy of the fluorescent species under study and τ_c is the correlation time.

Two main physical processes can lead to an apparent loss of anisotropy within the time window of the experiment.

(i) Rotational reorientation: The (photoselected) chromophores lose their alignment as a result of molecular motion and intermolecular collisions (with solvent molecules, etc.).

(ii) Energy migration: Energy is transferred to molecules which are not disposed vertically to the plane of polarization. This results in depolarization of the resultant emission.

In order to probe further the PNIPAMμgel system, preliminary time-resolved anisotropy measurements (TRAMS) were carried out below (25°C) and above (51°C) the LCST. It was hoped that such experiments would provide further information regarding the nature of the collapse of the nanoparticles and of the microviscosity within the hydrophobic domains created above the LCST.

Figure 5a shows the decays of fluorescence intensity of the components, $I_{\parallel}(t)$ and $I_{\perp}(t)$, from pyrene (10^{-6} *M*) dispersed within PNIPAMμgel (0.13 wt%) at 25°C. Reference to Fig. 5a reveals that $I_{\parallel}(t)$ and $I_{\perp}(t)$ converge rapidly within the time window accessed. In the current study, $r(t)$ has been analyzed directly (i.e., without any attempt to account for data distortion by the excitation pulse) and by impulse reconvolution (IR) [34,35]. [The latter method allows "deconvolution" of the $r(t)$ data, which is essential [36,37] if $r(t)$ decays on a time scale similar to the width of the excitation profile.] In the current study, $r(t)$ was adequately modeled by a single exponential function of the form of Eq. (5). A τ_c of ca. 1 ns results from both direct and IR analysis. This indicates that motion of the probe occurs on a rapid timescale. (Such would be expected within the fluid confines of the water-swollen, expanded particle below its LCST.) Above the LCST (51°C) the parallel and perpendicular components of pyrene's fluorescence do not fully converge within the time range shown (cf. Fig. 5b). The data provide a good graphic illustration of the effects of the restrictions imposed upon the rotational tumbling of the probe, constrained within the collapsed form of the microgel: this reflects the fact that a considerable degree of anisotropy persists until long times and infers that the pyrene experiences a very viscous environment compared to that encountered below the LCST. Use of a single-exponential function of the form of Eq. (5)

proved to be an adequate descriptor of the decay of anisotropy. A τ_c of ca. 1 μs was recovered by both direct and IR analysis.

The correlation time, τ_c, for a sphere rotating in a medium of viscosity, η, is related (see, for example, Ref. 1) to its volume, V, by Eq. (6):

$$\tau_c = \frac{\eta V}{RT} \tag{6}$$

A τ_c of ca. 1 μs, (as sensed by the probe) would infer (using a value of $\eta = 0.89$ cps for water, as the bulk medium at 298 K) that the diameter of the rotating entity is of the order of 21 nm.

This is smaller than the particle size (ca. 150-nm diameter) reported from light-scattering measurements from PNIPAM microgels synthesized by a high-temperature (70°C) method [16]. *If* the apparent dimensions of the tumbling probe (obtained from TRAMS) accurately reflect the true size of the microgel, then the temperature at which the polymerization is carried out markedly affects the nature of the resultant colloid. However, several other factors might serve to reduce the value of τ_c from that which might characterize the micro-Brownian rotation of an unperturbed microgel above its LCST.

(i) The solubilized pyrene guests may promote enhanced contraction of the gels through introduction of additional hydrophobic attractive forces within the particle interiors. (There is some spectroscopic evidence to suggest that organic probes can cause additional chain coiling when dispersed in certain water-soluble polymers [38].)

(ii) The interiors of the collapsed microgels might be of sufficiently low microviscosity and large enough dimension to allow restricted motion of the pyrene guests.

(iii) contraction of the microgels might reduce the apparent value of τ_c from that characteristic of the true value for the pyrene guest through the agency of energy migration from one chromophore to another: as the microgel particles collapse, the local guest concentration would increase, and although the chromophore density does not attain the levels required for excimer formation, energy transfers between pyrene moieties might become possible. The fact that estimates of the intrinsic anisotropy, r_o, recovered in impulse reconvolution analyses, are lower than anticipated for a distribution of isolated pyrene species [27] would support such conjecture.

Fluorescence studies in this area continue in our laboratories.

CONCLUSIONS

1. Luminescence techniques have proved useful in the study of the physical behavior of thermoresponsive microgels in aqueous dispersion. Fluorescence spectroscopy, quenching, and time-resolved anisotropy experiments, using pyrene as a probe, have revealed that PNIPAM nanoparticles collapse at the onset of the LCST. This phase transition occurs at ca. 38°C as sensed by fluorescence techniques.

2. Modification of the microgels, in the form of copolymerization with DMAC (i) shifts the LCST to a higher temperature; (ii) decreases the magnitude of the effect of the phase transition upon the photophysical characteristics of a dispersed pyrene probe, above the LCST, to an extent dependent upon the DMAC content of the microgel particles; and (iii) increases the degree of quenching effected by the addition of a neutral, water-soluble quencher (nitromethane) as observed above the LCST of the DMAC-modified microgel, to an extent dependent upon the amount of DMAC incorporated into the nanoparticles.

3. PNIPAM microgels have very compact hydrophobic interiors at temperatures in excess of 35°C. NIPAM–DMAC microgels, on the other hand, comprise more open, water-swollen structures above their respective LCSTs.

These observations reinforce those reported earlier on the basis of DSC and light-scattering experiments [17] that incorporation of the hydrophilic comonomer, DMAC, into the structure of the polymer forming the microgel raises its LCST and reduces the "intensity" of the transition associated with its volume collapse at the LCST. The novelty of the current work lies in the demonstration that such modification of the microgel network dramatically alters the nature of the microgel interiors above their respective LCSTs.

ACKNOWLEDGMENTS

The authors take pleasure in acknowledging financial support from the Leverhulme Trust (fellowship to N.J.F.) and are indebted to Ian Soutar for many interesting and stimulating discussions.

REFERENCES

1. K. P. Ghiggino and K. L. Tan (1985) in D. Phillips (Ed.), *Polymer Photophysics*, Chapman and Hall, London.
2. D. Y. Chu and J. K. Thomas (1984) *Macromolecules* **17**, 2142–2147.
3. J. A. Delaire, M. A. J. Rodgers, and S. E. Webber (1984) *J. Phys. Chem.* **88**, 6219–6227.
4. K. S. Arora and N. J. Turro (1987) *J. Polym. Sci. Polym. Phys. Ed.* **25**, 243–262.
5. J. J. Heyward and K. P. Ghiggino (1989) *Macromolecules* **22**, 1159–1165.
6. B. Bednar, J. Trnena, P. Svoboda, S. Vajda, V. Fidler, and K. Prochazka (1991) *Macromolecules* **24**, 2054–2059.
7. C. L. McCormick, C. E. Hoyle, and M. D. Clark (1991) *Macromolecules* **24**, 2397–2403.
8. I. Soutar and L. Swanson (1993) *Eur. Polym. J.* **29**, 371–378.
9. I. Soutar and L. Swanson (1994) *Macromolecules* **27**, 4304–4311.
10. M. Heskins, and J. E. Guillet (1968) *J. Macromol. Sci. Chem.* **A2**, 1441–1455.
11. F. M. Winnik (1990) *Macromolecules* **23**, 233–242.
12. F. M. Winnik (1990) *Polymer* **31**, 2125–2134.
13. R. Walter, J. Ricka, Ch. Quellet, R. Nyffenegger, and Th. Binkert (1996) *Macromolecules* **29**, 4019–4028.
14. C. K. Chee, S. Rimmer, I. Soutar, and L. Swanson (1997) *Polymer* **38**, 483–486.
15. L. D. Taylor and L. D. Cerankowski (1975) **13**, 2551–2570.
16. M. J. Snowden and B. Z. Chowdhry (1995) *Chem. Br.* **12**, 943–945.
17. M. Shibayama, S. Mitzutani, and S. Nomura (1996) *Macromolecules* **29**, 2019–2024.
18. M. J. Snowden, M. J. Murray, and B. Z. Chowdhry (1996) *Chem. Ind.* **7**, 531–534.
19. M. Murray, F. Rana, I. Haq, J. Cook, J, B. Z. Chowdhry, and M. J. Snowden (1994) *J. Chem. Soc. Commun.* **1994**, 1803–1804.
20. P. C. Griffiths, P. Stilbs, B. Z. Chowdhury, and M. J. Snowden (1995) *Colloid Polym. Sci.* **273**, 405–411.
21. M. J. Snowden, D. Thomas, and B. Vincent (1993) *Analyst* **118**, 1367–1369.
22. S. Pankasem, J. K. Thomas, M. J. Snowden, and B. Vincent (1994) *Langmuir* **10**, 3023–3026.
23. A. Nakajima (1970) *Bull. Chem. Soc. Jpn.* **43**, 967.
24. K. Kalyanasunderam and J. K. Thomas (1977) *J. Am. Chem. Soc.* **108**, 6270–6277.
25. F. M. Winnik (1993) *Chem. Rev.* **93**, 587–614.
26. D. M. Lucas, I. Soutar, and L. Swanson, unpublished data.
27. J. R. Ebdon, B. J. Hunt, D. M. Lucas, I. Soutar, L. Swanson, and A. R. Lane (1995) *Can. J. Chem.* **73**, 1982–1994.
28. J. B. Birks (1970) *Photophysics of Aromatic Molecules*, Wiley–Interscience, London.
29. D. Y. Chu and J. K. Thomas (1986) *J. Am. Chem. Soc.* **108**, 6270–6276.
30. A. F. Olea and J. K. Thomas (1989) *Macromolecules* **22**, 1165–1169.
31. M. A. Winnik, H. Zu, and R. Satguru (1993) *Makromol. Chem. Symp.* **70/71**, 107–117.
32. R. Satguru, J. McMahon, J. C. Padget, and R. C. Coogan (1994) *J. Coat. Technol.* **66**, 47–55.
33. I. Soutar, L. Swanson, T. Annable, J. C. Padget, and R. Satgurunathan, submitted for publication.
34. P. Wahl (1975) *Chem. Phys.* **7**, 220–228.
35. M. D. Barkley, A. A. Kowalczyk, and L. Brand (1981) *J. Chem. Phys.* **75**, 3581–3593.
36. I. Soutar (1992) *Makromol. Chem. Symp.* **53**, 393–409.
37. I. Soutar, L. Swanson, R. E. Imhof, and G. Rumbles (1992) *Macromolecules* **25**, 4399–4405.
38. L. Swanson (1989) Ph.D. thesis, Heriot-Watt University, Edinburgh, UK.